ISBN: 978-3-95450-262-2 ISSN: 2673-5350 doi: 10.18429/JACoW-IBIC2025-WEPCO09

BUNCH BY BUNCH MEASUREMENT AT THE HEPS BY OSCILLOSCOPE

J. He†,[1], F. Q. Huang[1], D. C. Zhu[1], Y. Zhao[1], T. G. Xu[1], Y. F. Sui[1,2], J.H. Yue[1], J.S. Cao[1,2]
[1] Institute of High Energy Physics Chinese Academy of Sciences, Beijing, China
[2] University of Chinese Academy of Sciences, Beijing, China

Abstract

By directly sampling beam position monitor (BPM) signals using a high-speed oscilloscope, individual bunches' transverse positions and longitudinal phases are resolved with unprecedented precision. A novel technique for extracting longitudinal phase information from oscilloscope data is detailed, achieving a resolution of 0.1 ps. Triggered by the injection timing signal, the oscilloscope captures transient dynamics during beam injection, enabling the derivation of critical parameters such as the longitudinal tune and residual oscillation amplitude, which are essential for optimizing injection efficiency. The injection processes of the High Energy Photon Source (HEPS) — spanning from the linear accelerator to the booster, from the booster to the storage ring, and subsequently from the storage ring back to the booster before re-entering the storage ring — have been thoroughly analysed and optimized using this method, demonstrating substantial potential for practical applications.

INTRODUCTION

The High Energy Photon Source (HEPS), China's first fourth-generation synchrotron radiation facility, commenced construction in July 2019 and is scheduled for completion in December 2025. During the first beam commissioning phase in the second half of 2024, the stored beam current in the storage ring exceeded 40 mA [1,2]. A critical milestone in beam store was fine-tuning the RF frequency, underscoring the interdependence of three key parameters: the RF frequency, beam energy from the booster, and beam energy set of the storage ring.

Most storage ring diagnostics—including orbit, betatron tune, and dispersion measurements—rely on turn-by-turn or multi-turn beam position data. However, bunch-by-bunch diagnostics provide far richer information. Acquiring transverse positions, longitudinal phases, and charge quantities for individual bunches is essential for understanding accelerator performance, particularly during initial commissioning.

Existing Bunch-by-bunch measurement systems fall into three categories: commercial bunch-by-bunch feedback systems [3], high-speed acquisition boards [4-5], and digital oscilloscopes [6-7]. Among these, the longitudinal phase reconstruction method developed by Prof. Leng's group at the Shanghai Synchrotron Radiation Facility (SSRF) has significantly expanded the applicability of oscilloscope data [8-9].

Commercial oscilloscopes are the most accessible hardware. With tailored algorithms, they can extract extensive accelerator parameters, including the equilibrium phase of bunches, the Phase oscillation amplitudes of injected bunches, the Synchrotron radiation damping coefficients, the Longitudinal tune, and others.

A distinctive feature of the HEPS, setting it apart from typical third- or fourth-generation light sources, is its beam reinjection system. In addition to on-axis injection from the booster to the storage ring, HEPS can kick low-charge bunches back to the booster, merge them with linac-supplied bunches to form higher-charge bunches, and then reinject them into the storage ring [10]. This process demands precise matching of RF systems (energy and phase) between the booster and storage ring.

DATA PROCESSING METHOD FOR BUNCH-BY-BUNCH LONGITUDINAL PHASE CALCULATING

In this study, BPM signals were acquired using two high-speed oscilloscopes: a Tektronix MSO64BW-6000 (6 GHz bandwidth, 25 GS/s maximum sampling rate) and a LeCroy 760Zi-A (20 GS/s maximum sampling rate). As illustrated in Fig. 1, signals from the BPMs are transmitted via 30-meter LMR-240 coaxial cables to the 6 GHz oscilloscope, synchronized with beam injection triggers. The HEPS employs dual radiofrequency systems operating at 166.6 MHz and 499.8 MHz, though only the 499.8 MHz system is presently operational. The bunch spacing is approximately two ns, and the harmonic number is 2268, with typical bunch charges around 1 nC.

The longitudinal phase of bunches could theoretically be resolved by sampling BPM signals at ultrahigh sampling rates. However, achieving a phase resolution of 0.1 ps would require a sampling rate of 10 THz—a currently unfeasible target due to hardware limitations and prohibitive data storage demands. The amplitude of the longitudinal oscillation of the newly filled bunch is several tens of picoseconds. The difference in equilibrium phases between different bunches is a few picoseconds. To study such issues, a resolution of 0.1 ps is mandatory. The non-integer ratio between the oscilloscope sampling rate and the RF frequency results in non-integer values for both N_{turn} and N_{rf}. During data concatenation, all sampled points $t_{\mathrm{sampling}}/(T_{\mathrm{rf}} \cdot t_0)$ are rounded to integers and assigned to their respective buckets and turns. For Steady-state studies where the BPM signal self-triggered acquisitions, bunch-filling verification is required only for the first turn. The first and last turns must be checked for injection-triggered acquisitions to identify newly injected bunches and their bucket numbers. Fig. 2(b) demonstrates the concatenated data of one bunch over 550 turns, yielding 27,500 points per RF period. This corresponds to an effective sampling rate of 13.75 THz (25 GHz × 550). Although these points are non-uniformly distributed, interpolation generates a standard

† hejun@ihep.ac.cn

Content from this work may be used under the terms of the CC BY 4.0 licence (© 2024). Any distribution of this work must maintain attribution to the author(s), title of the work, publisher, and DOI.

ISBN: 978-3-95450-262-2 ISSN: 2673-5350 doi: 10.18429/JACoW-IBIC2025-WEPCO09

Content from this work may be used under the terms of the CC BY 4.0 licence (© 2024). Any distribution of this work must maintain attribution to the author(s), title of the work, publisher, and DOI.

response function with uniform spacing at an equivalent 10-THz sampling rate.

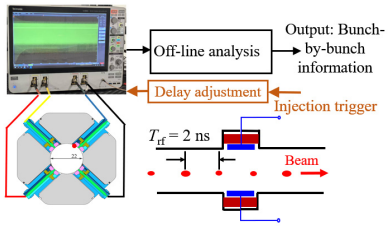

Figure 1: Schematic diagram of the bunch-by-bunch diagnostic system.

Upon obtaining the standard response function sampled at 10 THz, the 20,000 data points correspond to an RF phase, we temporarily define this phase as ϕ_0. Starting from the first point, a reference comparison table is constructed by extracting 50-point segments at intervals of 400 points. A cyclic permutation operation is then applied to the 20,000-point dataset, where the second data point is shifted to the first position, the third to the second, and the first to the 20,000th position. This rotation corresponds to a phase of ϕ_0 - 0.1 ps. Following the same procedure, a second 50-point reference table is generated. Repeating this process 20,000 times yields a lookup table (LUT) comprising 20,000 groups, each containing 50 points. Figure 2(c) illustrates representative reference tables (Groups 1, 5000, 10,000, and 15,000). The bunch-by-bunch data are cross-correlated with the LUT, and the group index yielding the highest correlation defines the bunch phase, denoted as ϕ_1 [8, 9]. The data processing workflow for longitudinal phase calculation is summarized in Table 1.

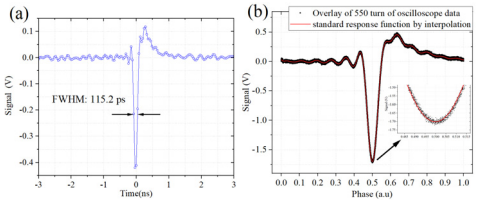

Figure 2: (a) The single-pass bunch signal captured by a 25 GS/s oscilloscope. (b) The stacked signal over 550 turns and the standard response signal are obtained by interpolation.

BUNCH-BY-BUNCH LONGITUDINAL PHASE RESULTS ANALYSIS

The phase data obtained from 2200 turns at a 6.25 GS/s sampling rate were fitted, with the fitting results shown by the red curve in Fig. 3(a). From this, we derived a longitudinal oscillation amplitude of 19.6 ps, a longitudinal tune of 0.00153 (corresponding to 654 turns per oscillation cycle), and a damping time of 18.1 ms (3991 turns), compared to the theoretical value of 18.7 ms. Compared to the 25 GS/s sampling rate results, the phase measurements at 6.25 GS/s exhibited greater jitter and uncertainty. To achieve longer-duration phase measurements, we conducted measurements using the Lecroy oscilloscope. The phase data and corresponding fit are shown in Fig. 3(b), revealing a longitudinal amplitude of 19.8 ps, a tune of 0.00097 (~1030 turns), and a damping time of 17.3 ms (3803 turns). The differences in the longitudinal working point and damping time between Fig. 3(a) and Fig. 3(b) arise from a shutdown period between the two measurements, during which multiple insertion devices were installed.

Table 1: The Data Processing Workflow for Longitudinal Phase Calculation

Step	Data size	Description
1. Origin data for bunch i at turn j	50 × 2 @25 GHz 20 × 2 @10 GHz	50 × 1 for the time, 50 × 1 for the signal strength.
2. Signal strength for bunch i at turn j	50 × 1 @25 GHz 20 × 1 @10 GHz	Only signal strength data were used
3. Multi-turn concatenation data for bunch i	27,500 × 1 @25 GHz 56,400 × 1 @10 GHz	50×550 @25 GHz 20×2820 @10 GHz.
4. Bunch referenced waveform	20,000 × 1 @0.1 ps	Interpolation processing to multi-turn concatenated data.
5. Table 3	20,000 × 20,000 @0.1 ps	20,000 successive cyclic permutations to bunch referenced waveform.
6. LUT	50 × 20,000 @25 GHz, 0.1 ps	Look up table
7. Correlation coefficient	1× 20,000 @25 GHz, 0.1 ps	The correlation between data in step *2* and step 6.
8. The best matching group	1×1	The index of maximum correlation coefficient for data in step 7.

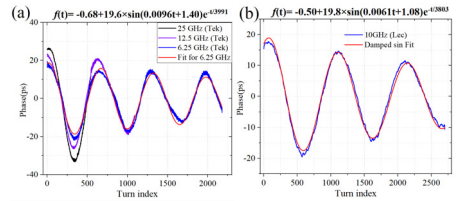

Figure 3: Longitudinal phase oscillation of the injection bunch with different (a) sampling rates and (b) oscilloscopes.

DIAGNOSIS OF BEAM LONGITUDINAL INSTABILITIES

Bunch-by-bunch data further enables the analysis of beam instabilities. Figure 4(a) displays the longitudinal phases of 60 bunches over 2820 turns (acquired by a LeCroy oscilloscope at 10 GHz), with a total beam current of 30.3 mA. The corresponding filling pattern and its

ISBN: 978-3-95450-262-2 ISSN: 2673-5350 doi: 10.18429/JACoW-IBIC2025-WEPCO09

charge are shown in Fig. 4(b). The highest-charge bunch (2753 pC) is at Bucket 1595 (Bunch 41), while Bunch 60 represents a newly injected bunch at the 119th turn. Fig. 4(a) shows that all bunches exhibit phase oscillations. Fig. 4(c) compares the phase evolution of Bunches 10, 20, 30, 40, 50, and 60, along with fitted curves for Bunches 50 and 60. Notably, no amplitude damping is observed for the stored bunches (excluding the newly injected one), justifying the use of a sinusoidal fitting function:

$$f(t) = y_0 + A\sin(\omega t + \phi_0) \quad . \qquad (1)$$

Figure 4(d) summarizes the fitting results for Bunches 1–59. The stored bunches' oscillation amplitudes are 11–20 ps, with a frequency around 0.00097 (normalized to the revolution frequency). For the injected bunch (Bunch 60), the oscillation amplitude is 33 ps and the frequency is 0.00087, indicating different dynamics.

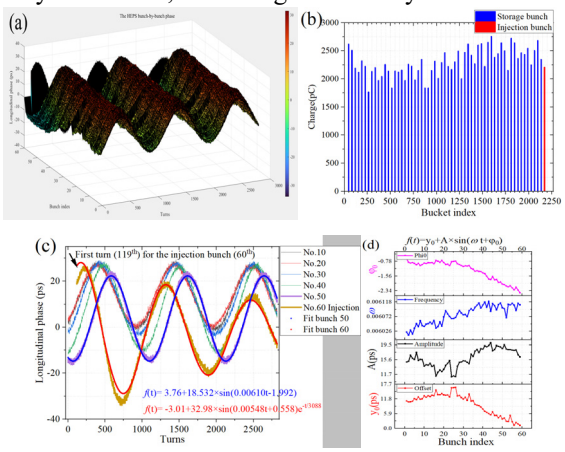

Figure 4: (a) The longitudinal phases of 60 bunches over 2820 turns. (b) The filling patterns and the bunch charges. (c) The phases of the storage/injection bunches with fitted curves. (d) The fitted parameter results for the storage bunches.

The results of the SVD analysis on the longitudinal phase data are presented in Fig. 5. Panels 13a, 13b, and 13c display the spatial vectors, temporal vectors, and frequency spectra of the first five modes, respectively, while 13d provides a detailed view of the low-frequency spectral region, with the corresponding singular values shown in the inset. The singular values of the first three modes are substantially larger than those of higher-order modes, indicating their dominant contributions to the beam dynamics. The SVD-reconstructed frequencies (Fig. 5(d)) show 0.00106 for Modes 1 & 2 (collective motion of all bunches) and 0.0071 for Mode 3 (driven primarily by the injected bunch).

The frequency resolution of the SVD is 0.0035, limited by the 2820-turn acquisition window, which explains minor discrepancies between fitted and SVD-derived frequencies. Mode 3 is unequivocally linked to the injected bunch, as evidenced by a jump in its temporal vector at Turn 119. As shown in Fig. 5(b), the evolution of the four-electrode sum signal determined the injection turn over multiple turns. It should be noted that, except for this measurement, the first mode is caused by the injected bunch in all our phase analysis results. Modes 1-2 represent global beam oscillations with contributions from all bunches. The higher frequency of Mode 3 (0.0071 vs. 0.00106 for Modes 1-2) reflects distinct dynamics of the injected bunch. The spectral broadening in Fig. 5(d) arises from the finite acquisition length, but the SVD still successfully isolates physically meaningful modes. The singular value ratios (inset, Fig. 5(d)) quantify the contribution energy of the mode. This analysis demonstrates the method's capability to resolve collective versus individual bunch dynamics, even with limited frequency resolution.

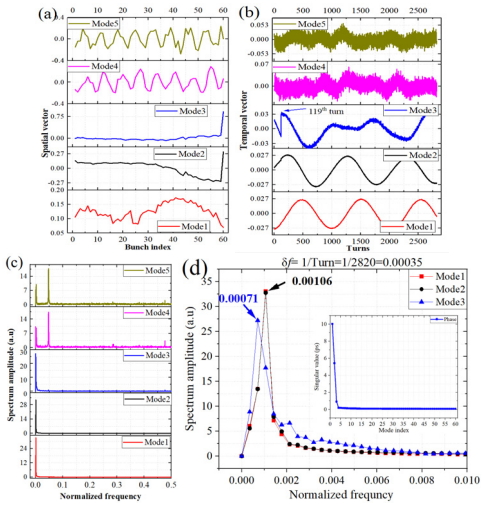

Figure 5: (a) Spatial eigenvectors, (b) temporal evolution profiles, and (c) FFT spectra of the first five SVD eigenmodes. (d) Zoomed view of low-frequency spectral components.

CONCLUSION

To address the diagnostic requirements during the initial commissioning phase of the HEPS, we have developed a bunch-by-bunch measurement system utilizing a BPM button pickup and a broadband oscilloscope. The longitudinal phase reconstruction follows the algorithm established by Leng et al., which enables precise determination of critical beam parameters including longitudinal tune, oscillation amplitude, and injection phase. A systematic implementation framework of this methodology is presented, with the derived parameters proving effective in optimizing injection efficiency. The application of the SVD analysis on the bunch-by-bunch dataset reveals its diagnostic power for identifying coupled-bunch instabilities, particularly through mode decoupling characteristics as shown in Fig. 4. The system's principal advantage lies in its cost-effectiveness and hardware simplicity, requiring only a standard oscilloscope (with sampling rate around 10 GHz for 500 MHz systems, and even lower specifications for lower RF frequencies) complemented by dedicated signal processing algorithms. Following the SSRF and Hefei Light Source, this methodology has been successfully implemented at the HEPS, demonstrating its potential for widespread application in various other types of accelerators.

Content from this work may be used under the terms of the CC BY 4.0 licence (© 2024). Any distribution of this work must maintain attribution to the author(s), title of the work, publisher, and DOI.

ISBN: 978-3-95450-262-2 ISSN: 2673-5350 doi: 10.18429/JACoW-IBIC2025-WEPCO09

© Content from this work may be used under the terms of the CC BY 4.0 licence (© 2024). Any distribution of this work must maintain attribution to the author(s), title of the work, publisher, and DOI.

REFERENCES

[1] H. Xu *et al.*, "First beam storage in the High Energy Photon Source storage ring", *Radiat. Detect. Technol. Methods*, vol. 9, pp. 70-81, 2025. doi:10.1007/s41605-024-00518-0

[2] Y. Jiao *et al.*, "The HEPS project", *J. Synchrotron Radiat.*, vol. 25, pp. 1611-1618, 2018. doi:10.1107/S1600577518012110

[3] iGp12 manual, Dimtel, Inc., US, 2025, https://www.dimtel.com/support/manuals/igp12

[4] M. G. Billing *et al.*, "Beam position monitoring system at CESR", *J. Instrum.*, vol. 12, pp. T09005, Sep. 2017.

[5] Y. Yang *et al.*, "Development of the bunch-by-bunch beam position acquisition system based on BEEcube", *Nucl. Sci. Tech.*, vol. 27, no. 47, 2016. doi:10.1007/s41365-016-0035-4

[6] J. Lee, M. H. Chun, G.-J. Kim, D.-C. Shin, D.-T. Kim, and S. Shin, "Bunch-by-bunch position measurement and analysis at PLS-II", *J. Synchrotron Radiat.*, vol. 24, pp. 163-167, 2017. doi:10.1107/S1600577516018154

[7] Y. Zhou, Z. Chen, B. Gao, N. Zhang, and Y. Leng, "Bunch-by-bunch phase study of the transient state during injection", *Nucl. Instrum. Methods Phys. Res. A* vol. 955, pp. 163273, 2020. doi:10.1016/j.nima.2019.163273

[8] X. Xu, Y. Leng, Y. Zhou, B. Gao, J. Chen, and S. Cao, "Bunch-by-bunch three-dimensional position and charge measurement in a storage ring", *Phys. Rev. Accel. Beams*, vol. 24, pp. 032802, 2021. doi:10.1103/PhysRevAccelBeams.24.032802

[9] X. Y. Xu *et al.*, "New non-invasive measurement method of optics parameters in a storage ring using bunch-by-bunch 3D beam position measurement data", *Phys. Rev. Accel. Beams*, vol. 24 pp. 062802, 2021. doi:10.1103/PhysRevAccelBeams.24.062802

[10] F. Liu *et al.*, "The design of HEPS global timing system", *Radiat. Detect. Technol. Methods.*, vol. 5, pp. 379-388, 2021. doi:10.1007/s41605-021-00257-6